



e-ISSN: 2319-8753 | p-ISSN: 2347-6710

IJIRSET

International Journal of Innovative Research in
SCIENCE | ENGINEERING | TECHNOLOGY

INTERNATIONAL JOURNAL OF INNOVATIVE RESEARCH

IN SCIENCE | ENGINEERING | TECHNOLOGY

Volume 12, Issue 8, August 2023

ISSN INTERNATIONAL
STANDARD
SERIAL
NUMBER
INDIA

Impact Factor: 8.423

9940 572 462

6381 907 438

ijirset@gmail.com

www.ijirset.com

Spectral and Raman Analysis of Er³⁺ Doped Ytterbium Zinc Lithium Sodalime Magnesium Borophosphate Glasses

S.L.Meena

Ceramic Laboratory, Department of Physics, Jai Narain Vyas University, Jodhpur (Raj.) India

ABSTRACT: Ytterbium zinc lithium sodalime magnesium borophosphate glasses containing Er³⁺ in (25-x):P₂O₅:10ZnO:10Li₂O:10CaO:10Na₂O:10MgO:10Yb₂O₃:15B₂O₃:xEr₂O₃ (where x=1, 1.5, 2 mol %) have been prepared by melt-quenching method. The amorphous nature of the glasses was confirmed by x-ray diffraction studies. Optical absorption, Excitation, Raman and Fluorescence spectra were recorded at room temperature for all glass samples. Judd-Ofelt intensity parameters Ω_λ ($\lambda=2, 4, 6$) are evaluated from the intensities of various absorption bands of optical absorption spectra. Using these intensity parameters various radiative properties like spontaneous emission probability, branching ratio, radiative life time and stimulated emission cross-section of various emission lines have been evaluated.

KEYWORDS: YZLSLMBP Glasses, Raman spectra, Judd-Ofelt Theory, Rare earth ions.

I. INTRODUCTION

Transparent glass ceramic as host materials for active optical ions have attracted great interest recently due to their potential application in solid state lasers, display devices, optical detector, lasers technologies and optical fiber amplifiers [1-5]. Oxide glasses are the most stable host matrices for practical applications due to their high chemical durability and thermal stability. Amongst many other glasses the P₂O₅ based glasses find wide spread applications in optical data transmission, detection and laser technologies. Phosphate glasses are very well known for their suitable mechanical and chemical properties, homogeneity, good thermal stability, and excellent optical properties phosphate glasses show an enhancement of rare earth radiative emission properties due to their variety of sites available for the doping ions [6-11]. Phosphate glasses have excellent transparency, good mechanical and thermal stability. Borophosphate glass has low phonon energy, chemical and thermal stability. Addition of ZnO improves chemical durability and thermal stability of the glasses [12]. Due to low melting point and glass transition temperature, preparations of borophosphate glasses are comparatively easier than other glass families [13-15].

The present work reports on the preparation and characterization of rare earth doped heavy metal oxide (HMO) glass systems for lasing materials. I have studied on the absorption, excitation, Raman and emission properties of Er³⁺ doped ytterbium zinc lithium sodalime magnesium borophosphate glasses. The intensities of the transitions for the rare earth ions have been estimated successfully using the Judd-Ofelt theory, The laser parameters such as radiative probabilities(A), branching ratio (β), radiative life time(τ_R) and stimulated emission cross section(σ_p) are evaluated using J.O.intensity parameters(Ω_λ , $\lambda=2, 4$ and 6).

II. EXPERIMENTAL TECHNIQUES

Preparation of glasses

The following Er³⁺ doped ytterbium zinc lithium sodalime magnesium boro phosphate glass samples (25-x):P₂O₅:10ZnO:10Li₂O:10CaO:10Na₂O:10MgO: 10Yb₂O₃:15B₂O₃:xEr₂O₃ (where x=1,1.5,2) have been prepared by melt-quenching method. Analytical reagent grade chemical used in the present study consist of P₂O₅, ZnO,



Li₂O, CaO, Na₂O, MgO, Yb₂O₃, B₂O₃ and Er₂O₃. All weighed chemicals were powdered by using an Agate pestle mortar and mixed thoroughly before each batch (10g) was melted in alumina crucibles in silicon carbide based an electrical furnace.

Silicon Carbide Muffle furnace was heated to working temperature of 1072⁰C, for preparation of ytterbium zinc lithium sodalime magnesium borophosphate glasses, for two hours to ensure the melt to be free from gases. The melt was stirred several times to ensure homogeneity. For quenching, the melt was quickly poured on the steel plate & was immediately inserted in the muffle furnace for annealing. The steel plate was preheated to 100⁰C. While pouring; the temperature of crucible was also maintained to prevent crystallization. And annealed at temperature of 350⁰C for 2h to remove thermal strains and stresses. Every time fine powder of cerium oxide was used for polishing the samples. The glass samples so prepared were of good optical quality and were transparent. The chemical compositions of the glasses with the name of samples are summarized in Table 1

Table 1 Chemical composition of the glasses

Sample	Glass composition (mol %)
YZLSLMBP (UD)	40P ₂ O ₅ :10ZnO:10Li ₂ O:10Al ₂ O ₃ :10Sb ₂ O ₃ :20B ₂ O ₃
YZLSLMBP (ER 1)	39P ₂ O ₅ :10ZnO:10Li ₂ O:10Al ₂ O ₃ :10Sb ₂ O ₃ :20B ₂ O ₃ :1 Er ₂ O ₃
YZLSLMBP (ER 1.5)	38.5P ₂ O ₅ :10ZnO:10Li ₂ O:10Al ₂ O ₃ :10Sb ₂ O ₃ :20B ₂ O ₃ : 1.5 Er ₂ O ₃
YZLSLMBP (ER 2)	38P ₂ O ₅ :10ZnO:10Li ₂ O:10Al ₂ O ₃ :10Sb ₂ O ₃ :20B ₂ O ₃ : 2 Er ₂ O ₃

YZLSLMBP (UD)—Represents Ytterbium Zinc Lithium Sodalime Magnesium Borophosphate glass specimen.

YZLSLMBP (ER) -Represents Er³⁺ doped Ytterbium Zinc Lithium Sodalime Magnesium Borophosphate glass specimens.

III. THEORY

3.1 Oscillator Strength

The intensity of spectral lines are expressed in terms of oscillator strengths using the relation [16].

$$f_{\text{expt.}} = 4.318 \times 10^{-9} \int \epsilon(\nu) d\nu \tag{1}$$

where, $\epsilon(\nu)$ is molar absorption coefficient at a given energy ν (cm⁻¹), to be evaluated from Beer–Lambert law.

Under Gaussian Approximation, using Beer–Lambert law, the observed oscillator strengths of the absorption bands have been experimentally calculated, using the modified relation [17].

$$P_m = 4.6 \times 10^{-9} \times \frac{1}{cl} \log \frac{I_0}{I} \times \Delta\nu_{1/2} \tag{2}$$

where c is the molar concentration of the absorbing ion per unit volume, l is the optical path length, log I₀/I is absorbivity or optical density and $\Delta\nu_{1/2}$ is half band width.



3.2. Judd-Ofelt Intensity Parameters

According to Judd [18] and Ofelt [19] theory, independently derived expression for the oscillator strength of the induced forced electric dipole transitions between an initial J manifold $|4f^N(S, L) J\rangle$ level and the terminal J' manifold $|4f^N(S', L') J'\rangle$ is given by:

$$\frac{8\pi^2 mc \bar{\nu}}{3h(2J+1)n} \frac{1}{n} \left[\frac{(n^2+2)^2}{9} \right] \times S(J, J') \tag{3}$$

where, the line strength S (J, J') is given by the equation

$$S(J, J') = e^2 \sum_{\lambda=2, 4, 6} \Omega_{\lambda} \langle 4f^N(S, L) J || U^{(\lambda)} || 4f^N(S', L') J' \rangle^2 \tag{4}$$

In the above equation m is the mass of an electron, c is the velocity of light, $\bar{\nu}$ is the wave number of the transition, h is Planck's constant, n is the refractive index, J and J' are the total angular momentum of the initial and final level respectively, Ω_{λ} ($\lambda = 2, 4$ and 6) are known as Judd-Ofelt intensity parameters.

3.3. Radiative Properties

The Ω_{λ} parameters obtained using the absorption spectral results have been used to predict radiative properties such as spontaneous emission probability (A) and radiative life time (τ_R), and laser parameters like fluorescence branching ratio (β_R) and stimulated emission cross section (σ_p).

The spontaneous emission probability from initial manifold $|4f^N(S', L') J'\rangle$ to a final manifold $|4f^N(S, L) J\rangle$ is given by:

$$A[(S', L') J'; (S, L) J] = \frac{64 \pi^2 \bar{\nu}^3}{3h(2J'+1)} \left[\frac{n(n^2+2)^2}{9} \right] \times S(J', J) \tag{5}$$

Where, $S(J', J) = e^2 [\Omega_2 || U^{(2)} ||^2 + \Omega_4 || U^{(4)} ||^2 + \Omega_6 || U^{(6)} ||^2]$

The fluorescence branching ratio for the transitions originating from a specific initial manifold $|4f^N(S', L') J'\rangle$ to a final manifold $|4f^N(S, L) J\rangle$ is given by

$$\beta[(S', L') J'; (S, L) J] = \sum_{S, L, J} \frac{A[(S', L) J']}{A[(S', L') J'; (\bar{S}, \bar{L}) \bar{J}]} \tag{6}$$

where, the sum is over all terminal manifolds.

The radiative life time is given by

$$\tau_{rad} = \sum_{S, L, J} A[(S', L') J'; (S, L) J] = A_{Total}^{-1} \tag{7}$$

where, the sum is over all possible terminal manifolds. The stimulated emission cross-section for a transition from an initial manifold $|4f^N(S', L') J'\rangle$ to a final manifold $|4f^N(S, L) J\rangle$ is expressed as

$$\sigma_p(\lambda_p) = \left[\frac{\lambda_p^4}{8\pi c n^2 \Delta \lambda_{eff}} \right] \times A[(S', L') J'; (\bar{S}, \bar{L}) \bar{J}] \tag{8}$$

where, λ_p the peak fluorescence wavelength of the emission band and $\Delta\lambda_{eff}$ is the effective fluorescence line width.

3.4 Nephelauxetic Ratio (β') and Bonding Parameter ($b^{1/2}$)

The nature of the R-O bond is known by the Nephelauxetic Ratio (β') and Bonding Parameters ($b^{1/2}$), which are computed by using following formulae [20, 21]. The Nephelauxetic Ratio is given by

$$\beta' = \frac{\nu_g}{\nu_a} \tag{9}$$

where, ν_a and ν_g refer to the energies of the corresponding transition in the glass and free ion, respectively. The value of bonding parameter ($b^{1/2}$) is given by

$$b^{1/2} = \left[\frac{1 - \beta'}{2} \right]^{1/2} \tag{10}$$

IV. RESULT AND DISCUSSION

4.1. XRD Measurement

Figure 1 presents the XRD pattern of the samples containing show no sharp Bragg's peak, but only a broad diffuse hump around low angle region. This is the clear indication of amorphous nature with in the resolution limit of XRD instrument.

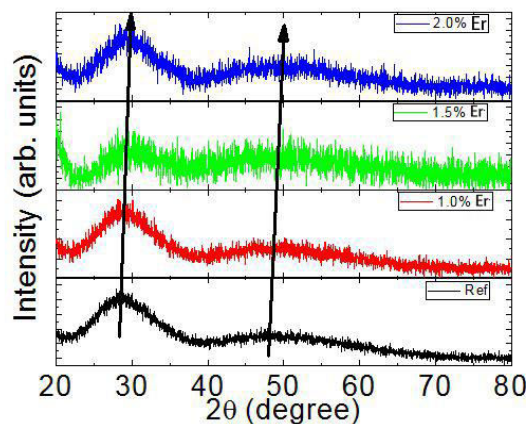


Fig.1: X-ray diffraction pattern of YZLSLMBP (ER) glasses.

4.2 Raman spectra

The Raman spectrum of Ytterbium Zinc Lithium Sodalime Magnesium Borophosphate (YZLSLMBP) glass specimens is recorded and is shown in Fig. 2. The spectrum peaks located at 397 and 779 cm^{-1} . The band at 397 cm^{-1} is related to the bending motion of phosphate polyhedral PO_4 units with cation like ZnO as the modifier. The broad band at 779 cm^{-1} is due to symmetric stretching of (P–O–P) bridging oxygen bonds in $(\text{P}_2\text{O}_7)_4$ units.

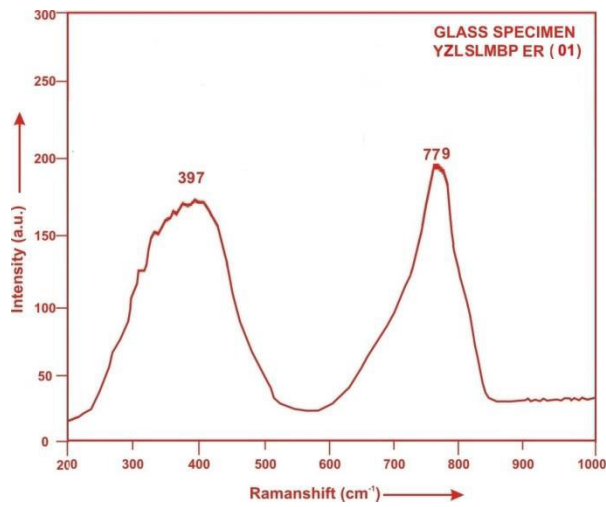


Fig.2: Raman spectra of YZLSLMP ER (01) glass.

4.3. Absorption spectra

The absorption spectra of YZLSLMBP (ER) glasses, consists of absorption bands corresponding to the absorptions from the ground state $^4I_{15/2}$ of Er^{3+} ions. Nine absorption bands have been observed from the ground state $^4I_{15/2}$ to excited states $^4I_{11/2}$, $^4I_{9/2}$, $^4F_{9/2}$, $^4S_{3/2}$, $^2H_{11/2}$, $^4F_{7/2}$, $^4F_{5/2}$, $^4F_{3/2}$, $^2H_{9/2}$ and $^4G_{11/2}$ for Er^{3+} doped YZLSLMBP (ER) glasses.

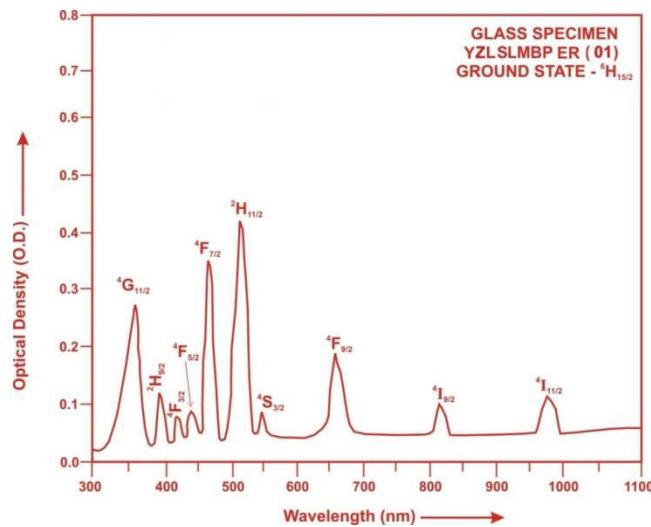


Fig.3: Absorption spectra of YZLSLMP ER (01) glass.

The experimental and calculated oscillator strengths for Er^{3+} ions in ytterbium zinc lithium sodalime magnesium borophosphate glasses are given in **Table 2**



Table 2. Measured and calculated oscillator strength ($P_m \times 10^{+6}$) of Er^{3+} ions in YZLSLMBP glasses.

Energy level $^4I_{15/2}$	Glass YZLSLMBP (ER01)		Glass YZLSLMBP (ER1.5)		Glass YZLSLMBP (ER02)	
	$P_{exp.}$	$P_{cal.}$	$P_{exp.}$	$P_{cal.}$	$P_{exp.}$	$P_{cal.}$
$^4I_{11/2}$	0.88	0.68	0.86	0.69	0.83	0.68
$^4I_{9/2}$	0.47	0.15	0.45	0.15	0.43	0.15
$^4F_{9/2}$	2.45	1.49	2.42	1.48	2.39	1.47
$^4S_{3/2}$	0.35	0.62	0.33	0.62	0.31	0.62
$^2H_{11/2}$	6.46	2.37	6.42	2.37	6.39	2.37
$^4F_{7/2}$	5.36	2.16	5.33	2.16	5.30	2.15
$^4F_{5/2}$	0.68	0.79	0.66	0.79	0.63	0.79
$^4F_{3/2}$	0.32	0.49	0.30	0.49	0.28	0.48
$^2H_{9/2}$	1.66	0.93	1.63	0.93	1.60	0.92
$^4G_{11/2}$	4.86	6.79	4.83	6.79	4.79	6.78
R.m.s.deviation	1.7995		1.7857		1.7771	

The various energy interaction parameters like Slater-Condon parameters F_k ($k=2, 4, 6$), Lande’s parameter ξ_{4f} and Racah parameters E^k ($k=1, 2, 3$) have been computed . The ratio of Racah parameters E^1/E^3 and E^2/E^3 are about 10.35 and 0.049 respectively. Computed values of Slater-Condon, Lande, Racah, nephelauxetic ratio and bonding parameter for Er^{3+} doped YZLSLMBP glass specimens are given in **Table 3**.

Table3. Computed values of Slater-Condon, Lande, Racah, nephelauxetic ratio and bonding parameter for Er^{3+} doped YZLSLMBP glass specimens.

Parameter	Free ion	YZLSLMBPER01	YZLSLMBP ER1.5	YZLSLMBP ER02
$F_2(cm^{-1})$	441.680	433.880	433.994	433.899
$F_4(cm^{-1})$	68.327	67.048	67.047	67.047
$F_6(cm^{-1})$	7.490	7.040	7.041	7.041
$\xi_{4f}(cm^{-1})$	2369.400	2414.815	2414.777	2414.777
$E^1(cm^{-1})$	6855.300	6661.485	6661.876	6661.875
$E^2(cm^{-1})$	32.126	31.335	31.338	31.338
$E^3(cm^{-1})$	645.570	643.691	643.685	643.685
F_4/F_2	0.15470	0.15453	0.15452	0.15452



F_6/F_2	0.01696	0.016225	0.016227	0.016227
E^1/E^3	10.61899	10.345	10.350	10.350
E^2/E^3	0.049764	0.04868	0.04868	0.048686
β'		0.99548	0.99555	0.99555
$b^{1/2}$		0.047517	0.047169	0.047168

Judd-Ofelt intensity parameters Ω_λ ($\lambda = 2, 4$ and 6) were calculated by using the fitting approximation of the experimental oscillator strengths to the calculated oscillator strengths with respect to their electric dipole contributions. In the present case the three Ω_λ parameters follow the trend $\Omega_4 < \Omega_2 < \Omega_6$. The values of Judd-Ofelt intensity parameters are given in **Table4**.

Table4. Judd-Ofelt intensity parameters for Er³⁺ doped YZLSLMBP glass specimens.

Glass Specimen	$\Omega_2(\text{pm}^2)$	$\Omega_4(\text{pm}^2)$	$\Omega_6(\text{pm}^2)$	Ω_4/Ω_6
YZLSLMBP (ER01)	0.8421	0.3214	0.9850	0.3263
YZLSLMBP (ER1.5)	0.8443	0.3151	0.9855	0.3197
YZLSLMBP (ER02)	0.8449	0.3136	0.9792	0.3203

4.4 Excitation Spectrum

The Excitation spectra of Er³⁺-doped YZLSLMBP (01) glass specimen has been presented in Figure 4 in terms of Excitation Intensity versus wavelength. The excitation spectrum was recorded in the spectral region 300–600 nm fluorescence at 550nm having different excitation band centered at 350,365, 381, 425, 455, 470 and 518 nm are attributed to the ²K_{15/2}, ⁴G_{9/2}, ⁴G_{11/2}, ²G_{9/2}, ⁴F_{3/2}, ⁴F_{5/2} and ²H_{11/2} transitions, respectively. The highest absorption level is ⁴G_{11/2} and is at 381nm. So this is to be chosen for excitation wavelength.

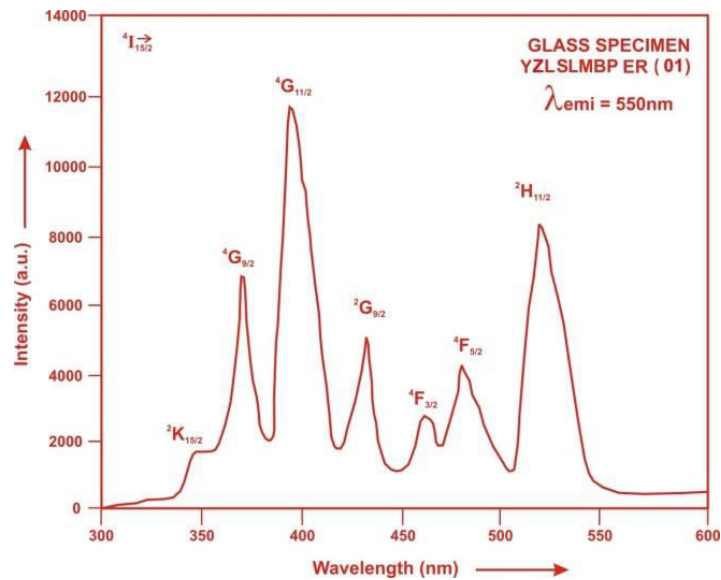


Fig.4: Excitation Spectrum of YZLSLMBP ER(01) glass.

4.5. Fluorescence Spectrum

The fluorescence spectrum of Er^{3+} doped in ytterbium zinclithium sodalime magnesium borophosphate glass is shown in Figure 5. There are six broad bands (${}^4F_{7/2} \rightarrow {}^4I_{15/2}$), (${}^2H_{11/2} \rightarrow {}^4I_{15/2}$), (${}^4S_{3/2} \rightarrow {}^4I_{15/2}$), (${}^4F_{9/2} \rightarrow {}^4I_{15/2}$), (${}^4I_{11/2} \rightarrow {}^4I_{15/2}$) and (${}^4I_{13/2} \rightarrow {}^4I_{15/2}$) respectively for glass specimens.

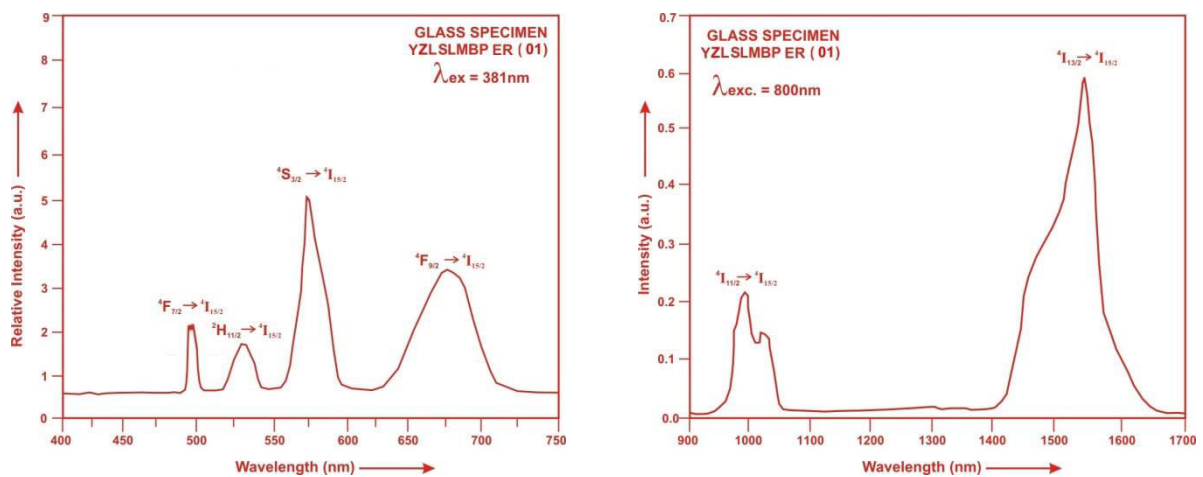


Fig.5: Fluorescence spectrum of YZLSLMBP ER (01) glass.

Table 5. Emission peak wave lengths (λ_p), radiative transition probability (A_{rad}), branching ratio (β_R), stimulated emission crosssection (σ_p), and radiative life time (τ) for various transitions in Er^{3+} doped YZLSLMBP glasses.

Transition	YZLSLMBP ER 01					YZLSLMBP ER 1.5				YZLSLMBP ER 02			
	λ_{max} (nm)	$A_{rad}(s^{-1})$	β	σ_p ($10^{-20} cm^2$)	$\tau_R(\mu s)$	$A_{rad}(s^{-1})$	β	$\sigma_p(10^{-20} cm^2)$	$\tau_R (\mu s)$	$A_{rad}(s^{-1})$	β	σ_p ($10^{-20} cm^2$)	τ_R ($10^{-20} cm^2$)
$^4F_{7/2} \rightarrow ^4I_{15/2}$ 2	485	1989.87	0.4111	0.5442	206.60	1993.08	0.4112	0.5342	206.33	1983.47	0.4106	0.5073	207.01
$^2H_{11/2} \rightarrow ^4I_1$ 5/2	530	1191.14	0.2461	0.3830		1192.82	0.2461	0.3740		1194.02	0.2472	0.3630	
$^4S_{3/2} \rightarrow ^4I_{15/2}$ 2	550	875.20	0.1808	0.2651		877.37	0.1810	0.2623		873.37	0.1808	0.2542	
$^4F_{9/2} \rightarrow ^4I_{15/2}$ 2	657	600.53	0.1241	0.3189		599.13	0.1236	0.3125		596.71	0.1235	0.3058	
$^4I_{11/2} \rightarrow ^4I_{15/2}$ 2	990	1013.91	0.0209	0.3543		1017.36	0.0210	0.3498		101.24	0.0210	0.3357	
$^4I_{13/2} \rightarrow ^4I_{15/2}$ 2	1538	82.158	0.0170	1.2377		82.366	0.0170	1.2261		81.96	0.0170	1.1869	

V. CONCLUSION

In the present study, the glass samples of composition $(40-x):P_2O_5:10ZnO:10Li_2O:10Al_2O_3:10Sb_2O_3:20B_2O_3:xEr_2O_3$ (where $x = 1, 1.5, 2$ mol %) have been prepared by melt-quenching method. The value of stimulated emission cross-section (σ_p) is found to be maximum for the transition ($^4I_{13/2} \rightarrow ^4I_{15/2}$) for glass YZLSLMBP (ER 01), suggesting that glass YZLSLMBP (ER 01) is better compared to the other two glass systems YZLSLMBP (ER1.5) and YZLSLMBP (ER02).

REFERENCES

- [1]. Seshadri, M., Radha, M., Bell, M.J.V. and Anjos, V. (2018). Structural and spectroscopic properties of Yb^{3+} doped porophosphate glasses for IR laser application. *Ceram. Int.* 44.20790-20797.
- [2]. Dousti, M.R., Poirier, G.Y. and de Camargo, A.S.S. (2020). Tungsten Sodium Phosphate glasses doped with trivalent rare earth ions (Eu^{3+} , Tb^{3+} , Nd^{3+} , Er^{3+}) for visible and near infrared applications, *Journal of Non-Cryst. Solids* 530, 119838.
- [3]. Dutchanephet, J., Dararutana, P. and Sirikulrat, N. (2017). UV-vis Spectroscopic and Dielectric Properties of Bismuth Borosilicate Glasses Doped with Potassium Chromate. *Chiang Mai J. Sci.* 44(3), 1083-1090.
- [4]. Marzouk, M.A., ElBatal, H.A., Hamdy, Y. M. and Ezz-Eldin, F.M. (2019). Collective Optical, FTIR and Photoluminescence Spectra of CeO_2 and/or Sm_2O_3 -Doped $Na_2O-ZnO-P_2O_5$ Glasses. *Int. J. Opt.* 6527327, 1-11.
- [5]. Vighnesh, K.R., Ramya, B., Nimitha, S., Wagh, A., Sayyed, M.I., Sakar, E., Yakout, H.A. and Dahshan, A. (2020). Structural, optical, thermal, mechanical, morphological and radiation shielding parameters of Pr^{3+} doped ZAIFB glass systems, *Optical materials* 99, 109512.

- [6].De, M. and Jana, S.(2020).Optical characterization of Eu^{3+} doped titanium barium lead phosphate glass,Optik-Int. Journal for light and Electron Optics,215,164718,1-7.
- [7]. Kumar,G.R. and Rao,C.S.(2020).Influence of Bi_2O_3 , Sb_2O_3 and Y_2O_3 on optical properties of Er_2O_3 -doped $\text{CaO-P}_2\text{O}_5\text{-B}_2\text{O}_3$ glasses, , Bull. Mater. Sci. 43:71,1-7.
- [8].Mandal, P.,Aditya,S.and Ghosh,S.(2020).Optimization of rare earth(Er^{3+}) doping level in lead zinc phosphate glass through Judd-Ofelt analysis, Mater.Chem. Phys. 246, 122802,1-7.
- [9].Chen, Y., Chen, G.H., Liu, X.Y. and Yang, T.(2018).Enhanced up – conversion luminescence and optical thermometry characteristics of $\text{Er}^{3+}/\text{Yb}^{3+}$ co-doped transparent phosphate Glass Ceramics, Journal of luminescence 195,314-320.
- [10]. Deepa, A.V., Priyamurygasen, P., Muralimanohar, K., Sathyamoorthy, and P., kumar, V. (2019) .A comparison on the structural and optical properties of different rare earth doped phosphate glass. Optik, 181,361-367.
- [11].Areej,S., Alqarni, S., Hussin, R., Alamri, S.N. and Ghoshal, S.K. (2020).Tailored structures and dielectric traits of holmium iondoped zinc-sulpho-boro-phosphate glass ceramics.Cerem. Int. 46(3), 3282-3291.
- [12] Sidek, H. A. A., Rosmawati, S., Azmi, B. Z. and Shaari, A. H. (2013). Effect of ZnO on the Thermal Properties of Tellurite Glass. Hindawi Publishing Corporation Advances in Condensed Matter Physics .1-6
- [13].Gorller-Walrand, C. and Binnemans, K. (1996). Handbook on the Physics and Chemistry of Rare Earths vol 23, ed K A Gschneidner Jr and L Eyring (Amsterdam: North-Holland) ch 155, p 121
- [14] Stokowski, S E, Saroyan R A and Weber M J (1981). Nd-Doped Laser Glass Spectroscopic and Physical Properties M-095, rev 2, vols 1 and 2 (Livermore, CA: Lawrence Livermore National Laboratory)
- [15].Zhang, L., Peng, M.,Dong,G. and Qiu,J.(2012).Spectroscopic properties of Sm^{3+} doped phosphate glasses, J. Mater. Res., 27, 16, 2111-2115.
- [16]. Gorller-Walrand, C. and Binnemans, K. (1988). Spectral Intensities of f-f Transition. In: Gshneidner Jr., K.A. and Eyring, L., Eds., Handbook on the Physics and Chemistry of Rare Earths, Vol. 25, Chap. 167, North-Holland, Amsterdam, 101.
- [17]. Sharma, Y.K., Surana, S.S.L. and Singh, R.K. (2009). Spectroscopic Investigations and Luminescence Spectra of Sm^{3+} Doped Soda Lime Silicate Glasses. Journal of Rare Earths, 27, 773.
- [18]. Judd, B.R. (1962). Optical Absorption Intensities of Rare Earth Ions. Physical Review, 127, 750.
- [19]. Ofelt, G.S. (1962). Intensities of Crystal Spectra of Rare Earth Ions. The Journal of Chemical Physics, 37, 511.
- [20].Sinha, S.P. (1983). Systematics and properties of lanthanides, Reidel, Dordrecht.
- [21].Krupke, W.F. (1974).IEEE J. Quantum Electron QE, 10,450.



INNO SPACE
SJIF Scientific Journal Impact Factor
Impact Factor: 8.423



ISSN INTERNATIONAL
STANDARD
SERIAL
NUMBER
INDIA



INTERNATIONAL JOURNAL OF INNOVATIVE RESEARCH

IN SCIENCE | ENGINEERING | TECHNOLOGY

9940 572 462 6381 907 438 ijirset@gmail.com



www.ijirset.com

Scan to save the contact details